

Gravity waves observed in temperature, wind and ozone data over Macquarie Island

Fabrice Chane-Ming

Laboratoire de Physique de l'Atmosphère, Université de la Réunion
and

Fiona Guest and David J. Karoly

School of Mathematical Sciences, Monash University, Australia

(Manuscript submitted April 2001; revised August 2002)

Characteristics of inertia-gravity waves are analysed in high-resolution vertical profiles of temperature, winds and ozone collected at Macquarie Island (54°S, 159°E) during the Airborne Southern Hemisphere Ozone Experiment/Measurements for Assessing the Effects of Stratospheric Aircraft (ASHOE/MAESA) observation programme in 1994. Two particular techniques are outlined to identify gravity-wave modes. The first is based on the continuous wavelet transform and seeks altitudes where the atmospheric fluctuations satisfy the gravity-wave polarisation relations in the temperature and wind soundings. The second analyses the phase and amplitude relationship of small-scale wavelike signatures seen in temperature and ozone profiles. The wavelet method identified gravity-wave modes with vertical wavelengths of 1-10 km, horizontal wavelengths of 50-1000 km and intrinsic frequencies of 1-2 f. Both methods reveal the presence of dominant modes with vertical wavelength <4 km in the upper troposphere and lower stratosphere over Macquarie Island. The energy activity of observed modes agrees well with the seasonal cycle of the upper level jet at 10 km height. These techniques together with classical spectral methods are applied to the case study of 25 October 1994 for which three quasi-monochromatic coherent modes with upwardly propagating wave energy are detected in the lower stratosphere.

Introduction

Knowledge of vertically-propagating gravity waves is crucial to understanding vertical transport and mixing

in the stratosphere and troposphere. As gravity waves propagate upwards from their sources, they interact with the background atmosphere modifying the dynamical structure, especially the large-scale circulation, and the distribution of chemical constituents of the atmosphere by means of wave transport and dissipation processes. Numerous studies have reported

Corresponding author address: Dr Fabrice Chane-Ming, Laboratoire de Physique de l'Atmosphère, Université de la Réunion, Faculté des Sciences et Technologies, 15 Av. René Cassin, BP 7151, 97715 Saint Denis Cedex 9, France. Phone: 262-262-93-82-39, Fax: 262-262-93-86-65

Email: fchane@univ-reunion.fr

signatures of small-scale vertical structures induced by gravity wave motions in the temperature, and wind fields and long-lived trace constituents of the atmosphere (Holton 1987, Teitelbaum et al. 1994, Grant et al. 1998; Pierce and Grant 1998). As a consequence, climate models and models of the chemistry of important trace constituents in the upper troposphere and lower stratosphere (UT/LS) have to correctly model the dynamics of such small-scale structures.

High-resolution radiosonde data collected by national meteorological agencies provide a large data set for the study of gravity-wave characteristics in the lower atmosphere on a global scale (Vincent et al. 1997). Several methods have been developed to extract and study the gravity wave signatures seen in radiosonde data (Vincent et al. 1997) in order to improve our knowledge of gravity wave processes and their parametrisation in global climate models (Hamilton 1997).

In this paper, we focus on two techniques to determine characteristics of quasi-monochromatic coherent vertical short-scale structures induced by gravity waves from ozonesonde and Omega wind-sounding data collected over Macquarie Island (Chane-Ming et al. 2000b, 2002). The first technique uses a method based on wavelet analysis and the second is based on the simplified analytical relation between the normalised perturbations of ozone and temperature. Results obtained using these techniques are compared with those obtained by Guest et al. (2000) using a classical spectral method applied to the case study of 25 October 1994.

Sounding data and preliminary data processing

High resolution upper-air Omega-sonde ozone soundings with Omega windsondes were carried out approximately weekly at Macquarie Island (54°S, 159°E) during the Airborne Southern Hemisphere Ozone Experiment/Measurements for Assessing the Effects of Stratospheric Aircraft (ASHOE/MAESA) programme in 1994. The mission involved the international collaboration of organisations from nine countries (including Australia), and was conducted to investigate the causes of ozone depletion in the wintertime middle latitudes in the southern hemisphere. The observational measurements used in the present study include 44 vertical profiles of temperature and horizontal wind for heights ranging between 0.5 km and a maximum altitude of 20-30 km. Corrected vertical profiles of ozone are available for 36 of the flights from the height of 1 km. The data were collected at 10 s intervals (corresponding to a spatial sampling of about 50 m) and are accurate to ± 0.2 K and 0.5 m s^{-1} for the temperature and the horizontal

winds respectively (Guest et al. 2000). Quality control was applied to the ozone measurements to improve their reliability. Thus some correction factors based on comparison with total column ozone measurements have been used for some flights. A precision of ± 3 per cent in ozone mixing ratio is measured by electrochemical concentration cell ozonesondes in the stratosphere below 10 hPa (Komhyr et al. 1995). Sampling of temperature, wind and ozone data are adjusted to 100 m vertical resolution using a cubic spline interpolation.

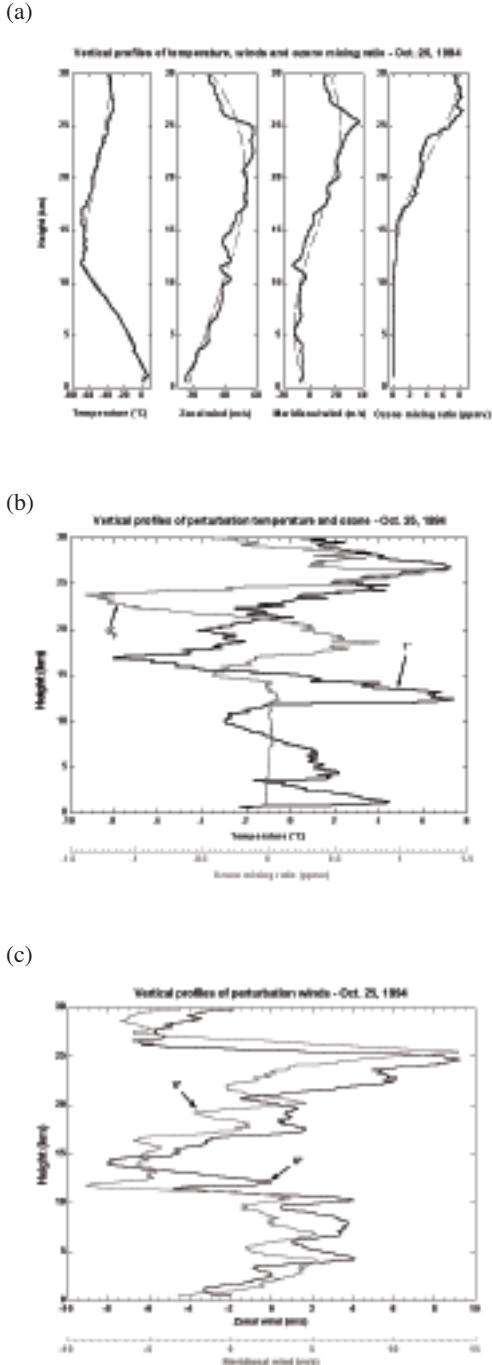
Small-scale fluctuations of temperature and horizontal winds are retrieved from individual raw vertical profiles using polynomial fits, in a least squares-sense, of order four and three respectively. In contrast, fluctuations of ozone concentration result from the application of a fourth order low-pass digital Butterworth filter with a cutoff of 7 km vertical wavelength (Mitchell et al. 1996). The extraction is improved, particularly around the tropopause, for the temperature when the filtering is applied separately below and above the tropopause corresponding to the troposphere and the stratosphere respectively. At the ends of the two vertical profiles, the filtering process is improved by a linear extrapolation of data (Chane-Ming et al. 2000b). Figure 1(a) shows vertical profiles of temperature, horizontal winds and ozone mixing ratio obtained on 25 October 1994 at Macquarie Island. The tropopause height is located at a height of 12 km on this day but typically varies between 8 and 12 km during 1994 (Guest et al. 2000). The extracted wavelike perturbations shown in Figs 1(b) and 1(c) are possible signatures of gravity waves.

Gravity wave analysis techniques

Wavelet method

In general terms, wavelet analysis measures the 'similarity' between the signal and basis functions called wavelets (Torrence and Compo 1998). Wavelets are scaled and translated versions of an oscillating 'mother' wavelet. In the Continuous Wavelet Transform (CWT), the scaled wavelet progressively moves along the time (or space)-varying signal and captures multiscaled structures in the signal. The characteristics of the CWT with Gaussian envelope, such as the complex-valued Morlet wavelet, were first outlined by Morlet et al. (1982) and Goupillaud et al. (1984) for the analysis of localised multiscaled structures in geophysics. This technique preserves amplitude (energy) and phase variations in time and proves to be well-adapted to the analysis of atmospheric gravity waves. Refer to Chane-Ming et al. (1999, 2000a) for a detailed description of the method, its mathematical properties, some applications of wavelets to gravity wave studies and references therein.

Fig. 1 (a) Vertical profiles of temperature, horizontal winds and ozone mixing ratio (solid lines) and the corresponding background profiles (dashed lines) on October 25, 1994. Perturbations of (b) temperature and ozone mixing ratio and (c) zonal and meridional winds.

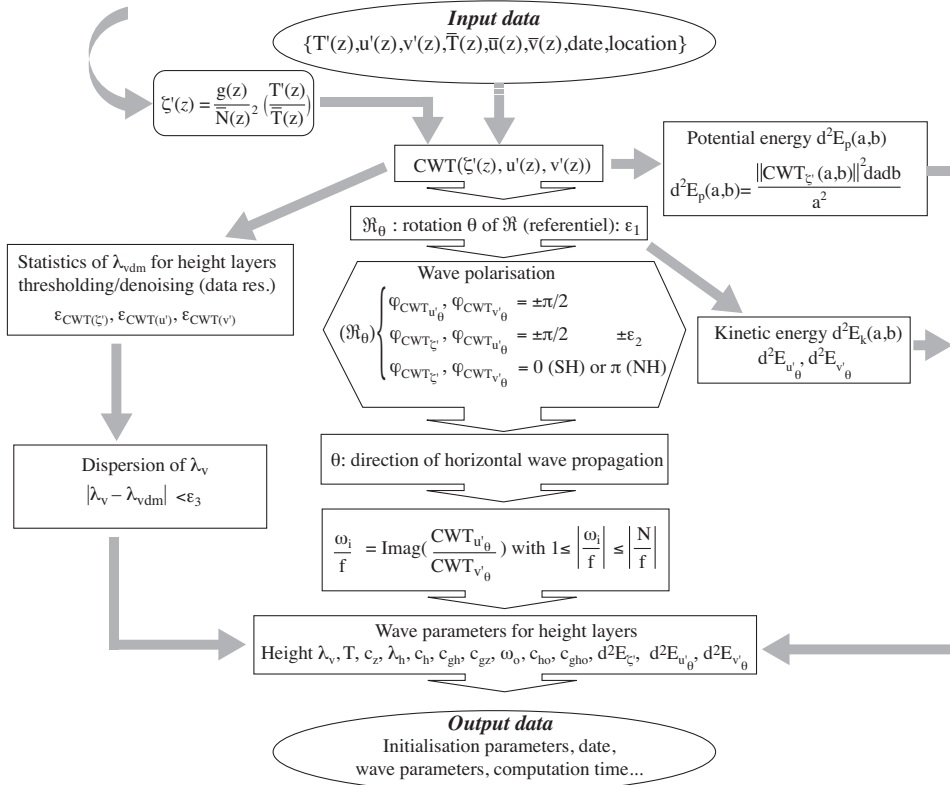


In this study, the CWT with the Morlet wavelet is applied to vertical profiles of perturbation temperature and winds to provide altitude-vertical wavelength information on small-scale structures embedded in each sounding with vertical wavelengths ranging between 0.6 and 10 km. Parameters such as energy, phase coherency, location in altitude and vertical wavelength, are directly extracted from the modulus and the phase of the CWT coefficients, and their location in the altitude-vertical wavelength plane. Like the modified Stokes' Parameter method (Eckerman and Vincent 1989; Guest et al. 2002), the polarisation relations for gravity waves (Gill 1982, p. 263), in the suitable coordinate system \mathfrak{R}_θ , where the abscissa is aligned with the horizontal direction of wave propagation, are used to retrieve coherent modes associated with gravity waves (Fig. 2). The iterative process consists of applying a rotation of the CWT planes of wind perturbations and calculating spectral parameters of detected coherent modes from the CWT coefficients. The horizontal direction of a coherent mode corresponds to the angle of rotation, θ , for which phase coherency is found; and the intrinsic frequency normalised by the inertial frequency, (ω_i/f) , is the ratio of the CWT_θ coefficients of the zonal and meridional wind perturbation. Intrinsic and ground-based horizontal spectral parameters are derived from the dispersion relation using the vertical wavelength, the intrinsic frequency and the background dynamical field (Gill 1982, Eqns 8.4.18, 8.4.24 and 8.4.26). A similar methodology was first utilised by Souprayen (1993).

A phase coherency uncertainty of 5° and 1° -step for rotation of \mathfrak{R} provide a good convergence of the statistics of the spectral parameter values. The statistics of the CWT spectra (Chane-Ming et al. 2000b, 2002) are calculated from the CWT coefficients of perturbations of each dynamical field (temperature, zonal and meridional wind) for several height layers. They determine the vertical wavelengths of dominant modes, λ_{vdm} , with a resolution of 0.5 km in vertical wavelength ranging between 0.5 and 11 km. Dominant modes detected in temperature and wind perturbations are selected with significant energy (≥ 10 per cent) relative to the CWT maximum values for three height layers (troposphere < 7 km, around the tropopause 7-13 km, LS 13-25 km). Possible effects of perturbations induced by the filtering of temperature around the tropopause are here limited to the height layer of 7-13 km. In addition the wavelet analysis distinguishes waves with different scales and thus separates coherent perturbations induced by gravity waves and those induced by the filtering.

Thresholding and noise-reduction methods enable us to select coherent modes with significant energy and in the neighbourhood of statistically observed

Fig. 2 Schematic description of the wavelet-based method for the extraction of gravity wave parameters of coherent modes. $\bar{T}(z)$, $\bar{u}(z)$, $\bar{v}(z)$, $\bar{N}(z)$ denote the background temperature, zonal and meridional winds and the static stability as a function of altitude z respectively; $T'(z)$, $u'(z)$, $v'(z)$ the perturbations; g the acceleration of gravity; (a, b) the scale and space parameter of the continuous wavelet transform (CWT); λ_v the vertical wavelength; λ_{vdm} the vertical wavelengths of dominant modes, φ the phase; f the inertial frequency; ω_i , ω_0 the intrinsic and apparent frequencies; T the period; c_{ho} , c_{gho} , c_h , c_{gh} the apparent and intrinsic horizontal phase and group velocities. Values of ε_1 , ε_2 and ε_3 are 1° , 5° and 0.5 km respectively.



dominant modes in the corresponding height layer. These methods reduce noise associated with measurements, the analysis, and the dispersion of highly-derived spectral parameters such as horizontal wavelength. Statistics of parameters of detected coherent modes are based on the ‘elementary’ total energy dE (Chane-Ming et al. 2000b) derived from the potential dE_p and kinetic energy dE_k (Fig. 2).

The advantage of the wavelet method lies in the linear expansion of coherent modes in an altitude-wavelength plane whereas conventional spectral analyses can only be applied to a restricted height range (Eckermann 1996). As opposed to the Fourier transform used in conventional spectral methods which provides a better resolution for detecting

modes with short vertical wavelengths, the wavelet method provides a good compromise between space and vertical-wavelength resolutions which improves the detection of modes with long vertical wavelengths. The wavelet method is based on the calculation of the phase coherency which could be biased when multiple structures interfere or side-effects at the two ends of the profiles and noise are important. In comparison the conventional spectral methods use continuous averaged power spectra in order to increase the confidence level or to reduce noise. Wavelet and conventional spectral methods rely on the assumption that the gravity wave field is made up of the superposition of dominant quasi-monochromatic coherent modes. Guest et al. (2002) showed a good

agreement in the detection of short vertical wavelengths by the wavelet and the modified Stokes' Parameter methods applied to the case of 27 March 1994. In addition GROGRAT, the ray-tracing model developed by Marks and Eckermann (1995), indicated that the longer modes with 5-6 km vertical wavelengths, detected by the wavelet method, could have originated from the same jet-front system as the shorter vertical wavelength modes.

Response of ozone to gravity-wave motions

The method is based on parcel advection by adiabatic gravity-wave motion, giving a simplified analytical relation between the normalised perturbations of ozone mixing ratio and temperature (Teitelbaum et al. 1994) :

$$\frac{O_3'(z,t)}{\bar{O}_3(z)} \approx R(z) \frac{T'(z,t)}{\bar{T}(z)} \quad \dots 1$$

$$\text{with } R(z) = \frac{1}{\bar{O}_3(z)} \frac{d\bar{O}_3(z)}{dz} \left(\frac{1}{\bar{\theta}(z)} \frac{d\bar{\theta}(z)}{dz} \right)^{-1} \quad \dots 2$$

\bar{O}_3 , O_3' denote the background and perturbation ozone mixing ratio; \bar{T} , T' the background and perturbation temperature; $\bar{\theta}$ the mean potential temperature and z the altitude. The phase and amplitude relationship between the normalised perturbations of ozone mixing ratio and temperature depends on the values of $R(z)$. The correlation between temperature and ozone enables us to distinguish between ozone laminae induced by Rossby and gravity waves (Teitelbaum et al. 1996; Gibson-Wilde et al. 1997; Pierce and Grant 1998). Chane-Ming et al. (2000b) used this equation to examine seasonal variations of vertical small-scale structures induced by gravity waves and horizontal large-scale advection across the subtropical barrier over La Réunion Island (21°S, 55°E). Eckermann et al. (1998) presented the basis of the parcel advection method and derived complete analytical formulae of the response of vertical constituent profiles to adiabatic gravity-wave motions. The normalised potential temperature perturbations agree with those of temperature.

Analysis results

First method

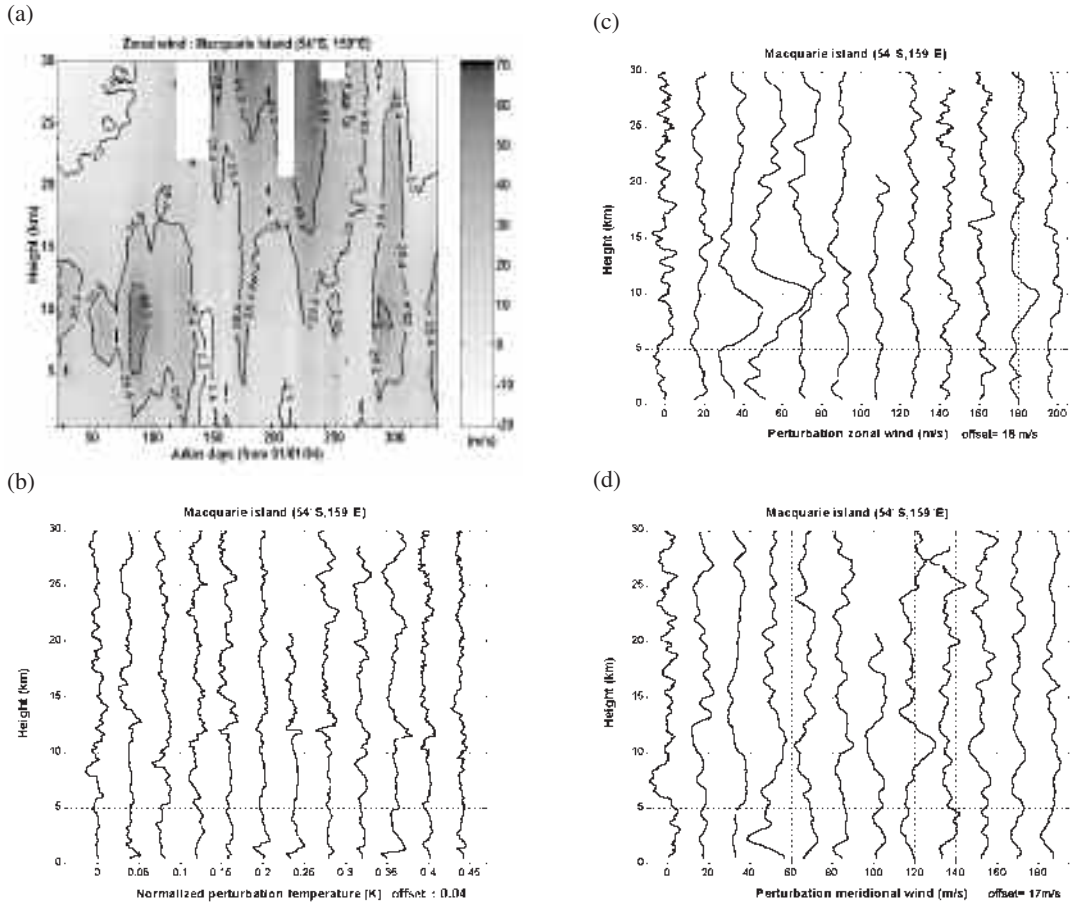
The wavelet method is applied to vertical profiles of temperature and horizontal winds for each sounding. Figure 3 shows the main input data for the wavelet method over the analysed time period. The zonal wind above 22 km height is eastward and strong during winter (May-August: Julian days 121-243) and

westward during summer (November-January: Julian days 305-031) (Vincent et al. 1997). In 1994, the transitional seasons are characterised by a strong upper level jet peaking at 10 km height with maximum intensities in April and October (Julian days: 91-121 and 274-304 respectively). Figures 3(b), 3(c) and 3(d) show the first vertical profiles of perturbation temperature and winds of each month for which ozone profiles are available.

Results of the wavelet method reveal the presence of coherent modes which are well-detected in the troposphere and the stratosphere. Dominant vertical wavelengths range between 1 and 10 km with horizontal wavelengths and intrinsic frequencies of 50-1000 km and 1-2 f respectively. Negative values of intrinsic frequencies normalised by the vertical wavenumber are indicative of an anticyclonic rotation of hodographs of wind perturbations which corresponds to upward propagation of wave energy in the southern hemisphere. They are observed to be dominant in the LS. In comparison Guest et al. (2000) found gravity-wave spectral characteristics ranging between 100 and 1000 km for the horizontal vertical wavelengths, between 1 and 7 km for the vertical wavelengths and between f and 2f for the intrinsic frequencies. Upward energy propagation was also found to be dominant in the LS but not in the troposphere. Results support the suggestion that sources of such waves are located in the troposphere (Guest et al. 2000).

Figure 4 (lower panel) shows the time-evolution of total energy per unit mass of coherent modes with 1-4 km vertical wavelengths and upward wave propagation energy for heights of 13-25 km provided by the wavelet analysis. The chosen altitude range eliminates the analysis of possible spurious wavelike structures induced by the filtering of temperature around the tropopause at heights of 8-12 km. Peaks coincide with maximum intensities of the upper tropospheric jet at 10 km height in March, April, August and October (Fig. 4 upper panel). The seasonal cycle agrees with the activity of the common synoptic pattern described by Guest et al. (2000) and with its minimum in winter (see Fig. 13 therein). One feature of this common synoptic pattern is the presence of an upper tropospheric jet and associated surface front lying upstream of Macquarie Island. The variance of wind perturbations is commonly used to analyse gravity wave activity (Guest et al. 2000). But it only works with the assumption that all extracted wavelike structures are induced by gravity waves. Therefore the presence of other types of wavelike structures or noise reduce the accuracy of this method. This is the drawback of the variance method as opposed to more sophisticated spectral methods such as the rotary spectral analysis and the wavelet method.

Fig. 3 (a) Vertical profiles of zonal winds over Macquarie Island during 1994. Crosses on the horizontal axis locate the 44 observations with 100 m spatial resolution, 36 of which include ozone data, (grey crosses). (b) Vertical profiles of perturbations of temperature normalised to the background temperature, (c) perturbations of zonal winds and (d) meridional winds, associated with the first vertical profiles of ozone of each month (12 profiles). Profiles are successively offset by 0.04 K, 18 m/s and 17 m/s for the normalised temperature perturbations, the zonal and meridional wind perturbations, respectively.

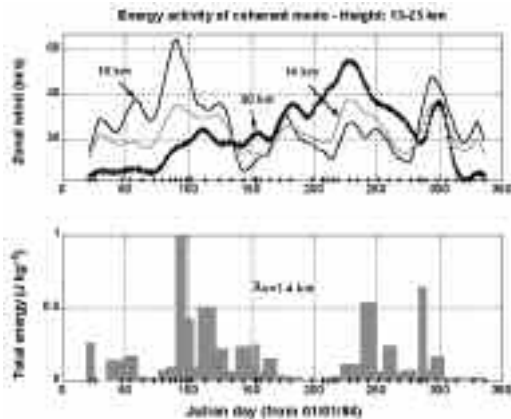


Second method

Perturbations of normalised temperature and ozone are combined to identify signatures of gravity waves when corrected 1994 ozone data are available. Figure 5 shows vertical profiles of raw ozone concentration in 1994 and the first vertical profiles of normalised ozone mixing ratio perturbations (one for each month). The seasonal evolution shows maximum ozone concentrations at heights between 15 and 25 km with the largest values occurring in late winter. Refer to Bojkov et al. (1998) for details on ozone trends in relation to observed ozone depletion. In addition, for the height range 20–25 km, minimum values are observed in March and April.

Normalised ozone mixing ratio and temperature perturbations show small-scale wavelike structures in the UT/LS (Fig. 3(b) and 5(b)). As mentioned in the discussion of Eqn 1, the comparison of amplitude and phase of normalised ozone perturbations with those of normalised temperature perturbations, which have been multiplied by the $R(z)$ coefficients (smoothed over 2.5 km), indicates whether gravity-wave signatures are present in the profiles. Thus the phase relationship depends on the sign of $R(z)$ which varies with height due mainly to the variation of the vertical gradient of background ozone. The coefficient $R(z)$ is globally positive (negative) throughout most of the

Fig. 4 Time series of the intensities of the zonal wind at heights of 10, 14 and 20 km (upper panel). Time-evolution of total energy per unit mass of the modes with 1–4 km vertical wavelengths and upward wave propagation energy ($\omega/m < 0$) in the stratosphere for heights of 13–25 km (lower panel). The energy is normalised by the maximum value of the analysed period.



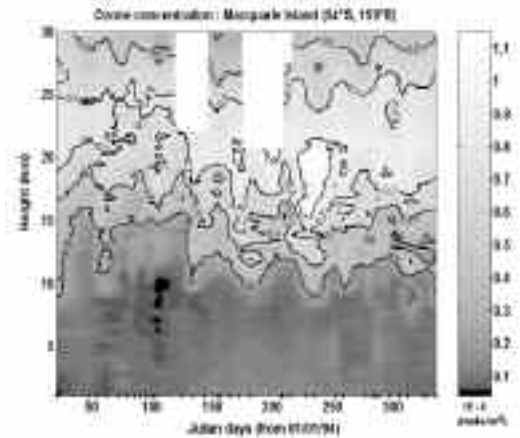
troposphere in summer (winter) with absolute values < 30 . Positive values < 40 (60) are found above the tropopause in the LS in summer (winter). Small values of $R(z)$ are observed in the stratosphere above 20 km height where the vertical gradient of ozone mixing ratio is small. Wavelike structures with vertical wavelengths of 1–4 km are extracted from each part of Eqn1 with the use of a fourth order bandpass digital Butterworth filter. Correlation coefficients are calculated with a 3 km window (Fig. 6). Perturbations are observed to be well-correlated in the UT/LS with correlation values > 0.7 , especially during April and May. This is partly due to wave interferences in the troposphere and the wave filtering effect of the background wind. Correlation is less important where the upper level jet is intense due to the simultaneous presence of small-scale structures induced by large-scale advection and gravity waves. Note that many quasi-monochromatic structures induced by gravity waves with both upward and downward progression energy could also interfere and produce biased correlation values. Thus the second method is more efficient when analysing individual soundings because the filtering process can be improved to focus on observed dominant quasi-monochromatic modes as described below in the case study of 25 October 1994.

Case study of 25 October 1994

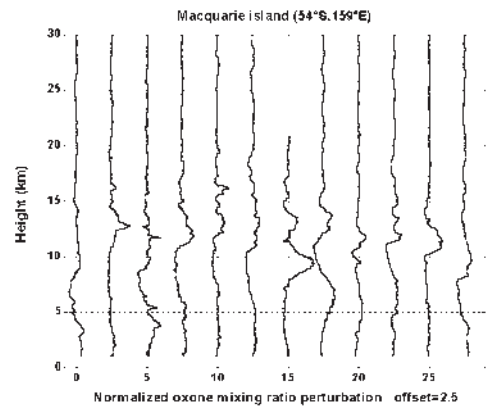
Guest et al. (2000) presented a case study of 25 October 1994 (Fig. 1) for which the source of domi-

Fig. 5 (a) Vertical profiles of ozone concentration (moles/m³) for 36 soundings over Macquarie Island in 1994. (b) First vertical profiles of normalised ozone mixing ratio perturbations of each month (12 profiles) successively offset by 2.5.

(a)

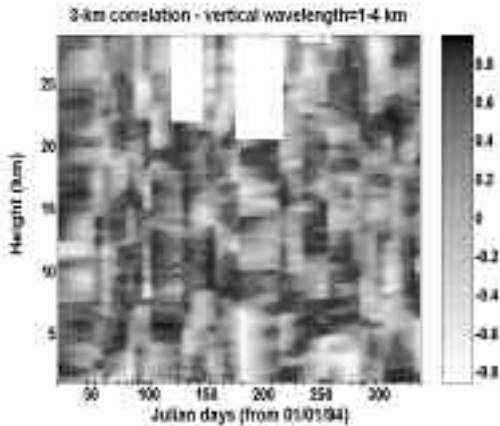


(b)



nant gravity waves observed at heights between 13.5–28.5 km was investigated with a ray-tracing model developed by Marks and Eckermann (1995). Rays were initialised at 21 km height and traced backwards through the upper level jet to the vicinity of a cold front. Methods presented in this study are applied to that case study for a comparison of results. Figure 7(a) visualises the distribution of vertical wavelengths versus height for dominant coherent modes detected in the troposphere and the stratosphere by the wavelet-based method. Coherent modes with 2 km, 3-

Fig. 6 Correlation between normalised perturbations of temperature (Fig. 3(b)) and ozone mixing ratios (Fig. 5(b)) for 36 observations over Macquarie Island in 1994: 3 km correlation coefficients for wavelike structures of ozone and temperature with 1-4 km vertical wavelengths. Profiles of normalised temperature perturbations have been multiplied by the 2.5-km smoothed profiles of $R(z)$. Contours indicate values of 0.5 and 0.7.

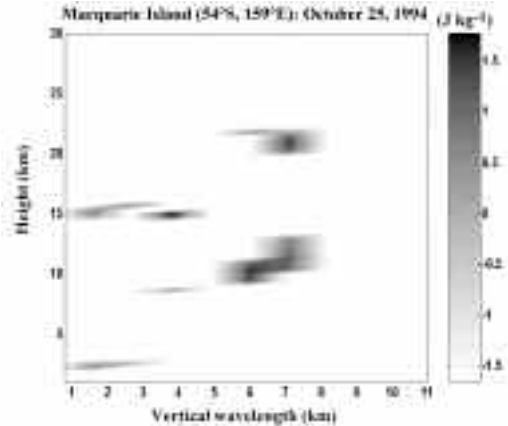


4 km and 6-7 km vertical wavelengths are observed in the stratosphere in the height range 13-28 km (Fig. 7(b)). The method detects a coherent mode only if its vertical extension is about that of the vertical wavelength for the mode with long vertical wavelength (7 km) and triple or twice for the short vertical wavelength (1-2 km). The analysis shows that the phase coherency of the energetic mode with 7 km vertical wavelength is better at 21 km which indicates that the wave is located between 18.5-24.5 km. The energy above 25 km is small because the phase coherency is affected by side effects induced by the wavelet method at the upper part of the profile. Thus the increase of the phase coherency uncertainty enables us to detect the quasi-monochromatic wave with 6-7 km vertical wavelengths between 20 and 30 km observed in the hodograph of the horizontal perturbation wind (Guest et al. 2000). In addition, similar results are obtained when the wavelet method is applied to the whole vertical profile up to 35 km as in the case of 25 October 1994.

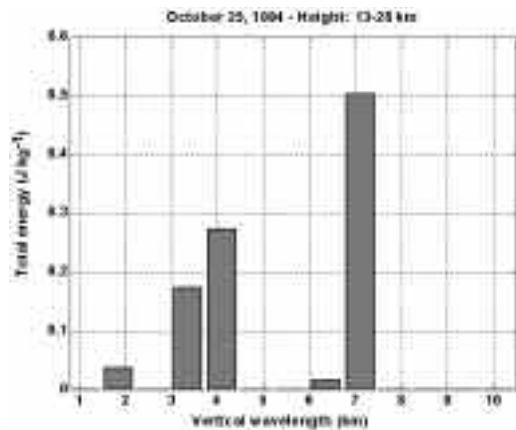
Figure 8(a) represents the correlation between perturbations of normalised temperature and ozone mixing ratio for 0.5-7 km vertical wavelengths provided by the second method. Temperature perturbations have been multiplied by the 2.5 km smoothed profile of $R(z)$ (Fig. 8(a) second panel). Evidence of similar

Fig. 7 (a) Distribution of total energy per unit mass in logarithmic scale of coherent gravity-wave modes on a height-vertical wavelength plane detected in the 25 October 1994 sounding. (b) The corresponding normalised histogram versus vertical wavelengths at heights between 13-28 km.

(a)



(b)



wavelike structures is shown with a good relationship between amplitudes and phases at heights of 8-14 km (Fig. 8a first and last panels). At heights between 8 and 14 km, absolute values of the normalised amplitude extrema are superior to the precision of ± 3 per cent in the ozone mixing ratio and the correlation coefficients are >0.7 . The ± 3 limits enable us to detect possible laminated structures induced by horizontal large scale advection (Fig. 8(a) last panel). We conclude that the observed wavelike structures can be attributed to gravity waves (Pierce and Grant 1998).

Fig. 8 (a) Normalised perturbations of the temperature and the ozone mixing ratio (gray and black curves respectively in the first panel) on October 25, 1994, for the vertical wavelength bandwidth of 0.5-7 km; the vertical gray lines indicate the 3 per cent instrumental precision in the ozone mixing ratio; the vertical profile of normalised temperature has been multiplied by the 2.5-km smoothed profile of $R(z)$ (second panel). The 3km-correlation (black curve) and values of ± 0.3 and 0.7 (gray lines) are represented in the third panel. (b) Same as Fig. 8(a) (first panel) but for vertical wavelengths of 2-3 (first panel), 3.5-4.5 (second panel) and 5-7 km (third panel).

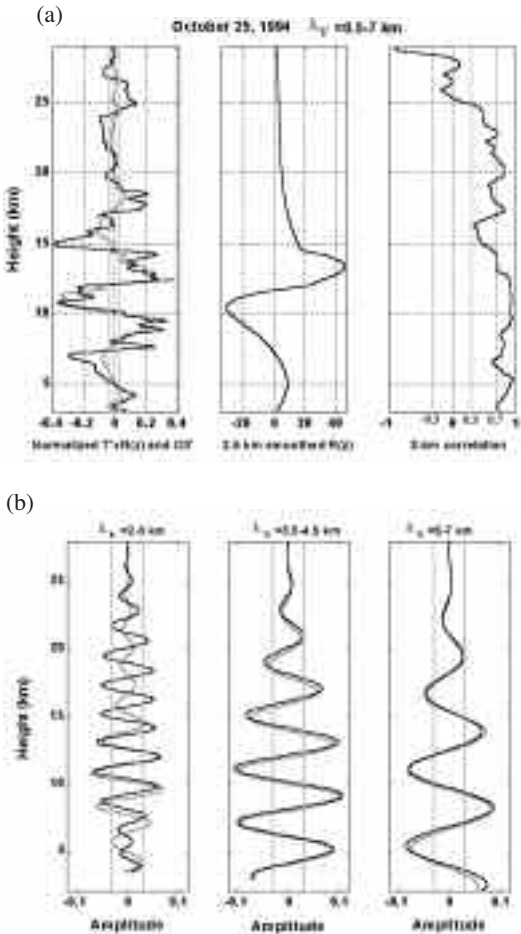
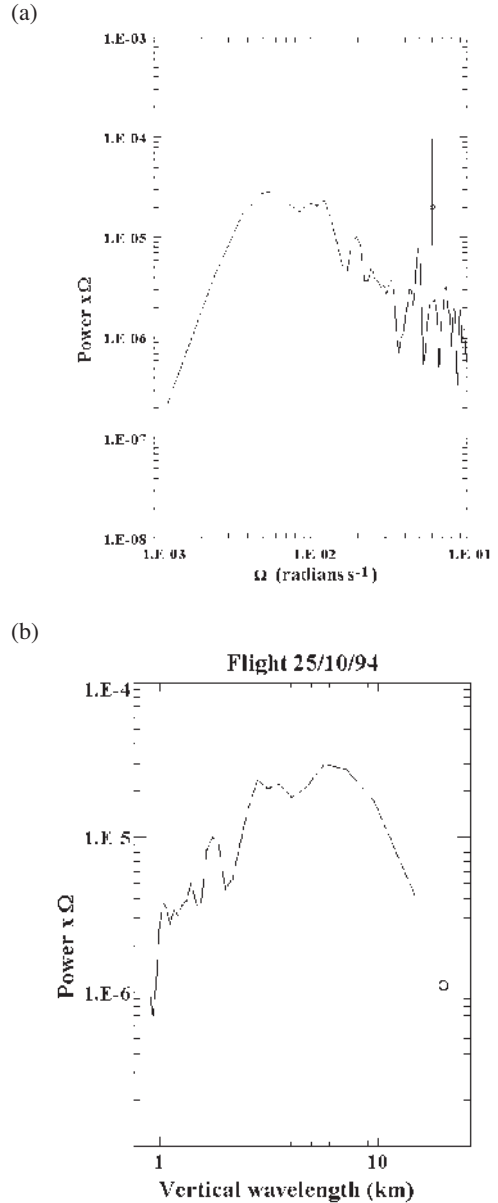


Fig. 9 Standard spectral analysis on October 25, 1994 for 12-30 km height: (a) temperature power spectrum as a function of the apparent frequency Ω ; (b) the corresponding vertical wavelength power spectrum. Error bars indicate the 95 per cent confidence levels.



The extraction of the dominant mode is improved for vertical wavelengths of 2-3 km, 3.5-4.5 km and 5-7 km (Fig. 8(b)). Signatures of wavelike structures are well-correlated both in amplitudes and phases at heights above 3 km although the sign of $R(z)$ changes

at heights of 7 km and 12 km. (Fig. 8(b) second and third panels). This method also works well for waves with 2-3 km vertical wavelengths but only at heights between 10 and 14 km (Fig. 8(b) first panel). This method cannot detect signatures of gravity waves with significant amplitudes above 20 km height

because of small values of $R(z)$ (Fig. 8(a) first panel and 8(b)) as mentioned in Chane-Ming et al. (2000b). Figure 4 in Guest et al. (2000) which represents the rotary spectra for 25 October 1994 as a function of the apparent frequency, Ω , shows upward energy propagation is observed to be dominant in the stratosphere at heights between 12 and 30 km. A comparison of the peaks of the rotary spectrum with the corresponding temperature power spectrum shows good agreement (Fig. 9(a)). Guest et al. (2000, Eqn 6) is used to determine the temperature power spectrum as a function of vertical wavelength (Fig. 9(b)). Figure 9(b) reveals the presence of dominant stratospheric modes with vertical wavelengths of 1.7 km, 3-4 km and 6-7 km. These agree well with those identified using the two methods of this study.

Conclusion

This study has used two additional techniques to complete the analysis of gravity waves detailed by Guest et al. (2000) at Macquarie Island (54°S, 159°E) in 1994. The first method, based on wavelet decomposition, has determined the characteristics of gravity waves in temperature and wind profiles similar to the study of Guest et al. (2000) which used a classical spectral method. In addition the second method has analysed ozone data to obtain information on gravity waves. The two methods produced additional and consistent results on the characteristics of gravity waves and the energy activity in agreement with the climatology of a common synoptic pattern (Guest et al. 2000). These techniques together with classical spectral methods have been applied to the case study of 25 October 1994. They have shown clear evidence of the presence of three quasi-monochromatic structures induced by gravity waves in the LS. In addition the second method has also revealed the presence of these structures in the troposphere. The advantages and weaknesses of the two methods have been discussed in comparison with classical spectral methods. In conclusion, this study illustrates the usefulness of high-resolution balloon data (temperature, winds and ozone measurements) for the analysis of gravity wave motions in the troposphere and lower stratosphere.

Acknowledgments

The scientific collaboration between the Laboratoire de Physique de l'Atmosphère (LPA) and the Cooperative Research Centre for Southern Hemisphere Meteorology (CRCSHM) was possible thanks to Prof. D. J. Karoly and Prof. J. Leveau with financial support from La Région Réunion/l'Europe.

Additional thanks are due to J. Easson from the Atmosphere Watch section of the Australian Bureau of Meteorology who provided the data set and the two anonymous reviewers for helpful and constructive comments on the manuscript.

References

- Bojkov, R.D. and Hudson, R.D. 1998. Ozone variability and trends. In: Scientific Assessment of Ozone Depletion: 1998. WMO *Global Ozone Research and Monitoring Project. Report No. 44*, Geneva.
- Chane-Ming, F., Molinaro, F. and Leveau, J. 1999. Wavelet techniques applied to lidar signal in the analysis of the middle atmosphere dynamics. *Appl. Signal Process.*, 6, 94-104.
- Chane-Ming, F., Molinaro, F., Leveau, J., Keckhut, P. and Hauchecorne, A. 2000a. Analysis of gravity waves in the tropical middle atmosphere with lidar using wavelet techniques. *Ann. Geophys.*, 18, 485-98.
- Chane-Ming, F., Molinaro, F., Leveau, J., Keckhut, P., Hauchecorne, A. and Godin, S. 2000b. Vertical short-scale structures in the upper tropospheric-lower stratospheric temperature and ozone at La Reunion Island (20.8°S, 55.3°E). *J. geophys. Res.*, 105, 26,861-6.
- Chane-Ming, F., Roff, G., Robert, L. and Leveau, J. 2002. Gravity wave characteristics over Tromelin Island during the passage of cyclone Hudah. *Geophys. Res. Lett.*, 29, 10.1029/2001GL013286.
- Eckermann, S.D. and Vincent, R.A. 1989. Falling sphere observations of anisotropic gravity wave motions in the upper stratosphere over Australia. *Pure Appl. Geophys.*, 130, 509-32.
- Eckermann, S.D. 1996. Hodographic analysis of gravity waves: relationships among Stokes' parameters, rotary spectra and cross-spectral methods. *J. geophys. Res.*, 101, 19,169-74.
- Eckermann, S.D., Gibson-Wilde, D.E. and Bacmeister, J.T. 1998. Gravity wave perturbations of minor constituents: A parcel advection methodology. *J. Atmos. Sci.*, 55, 3521-39.
- Gibson-Wilde, D.E., Vincent, R.A., Souprayen, C., Godin, S., Hertzog, A. and Eckermann, S.D. 1997. Dual lidar observations of mesoscale fluctuations of ozone and horizontal winds. *Geophys. Res. Lett.*, 24, 1627-30.
- Gill, A.E. 1982. *Atmosphere-Ocean Dynamics*. Academic Press Inc., 622 pp.
- Goupillaud, P., Grossmann, A. and Morlet, J. 1984. Cycle-octave and related transforms in seismic signal analysis. *Geoexploration*, 23, 85-102.
- Grant, W.B., Pierce, R.B., Oltmans, S.J. and Browell, E.V. 1998. Seasonal evolution of total and gravity wave-induced laminae in ozonesonde data in the tropics and subtropics. *Geophys. Res. Lett.*, 25, 1863-6.
- Guest, F.M., Reeder, M.J., Marks, C.J. and Karoly, D.J. 2000. Inertia-gravity waves observed in the lower stratosphere over Macquarie Island. *J. Atmos. Sci.*, 57, 737-52.
- Guest, F.M., Reeder, M.J., and Chane-Ming, F. 2002. Analyses of inertia-gravity waves in upper-air soundings made from Macquarie Island. *Aust. Met. Mag.*, 51, 107-15.
- Hamilton, K. 1997. *Gravity wave processes: their parameterization in global climate models*. Springer-Verlag, 404 pp.
- Holton, J.R. 1987. The production of temporal variability in trace constituent. *Proceedings of the NATO Advanced Research Workshop on Transport Processes in the Middle Atmosphere*, Erice, Italy, November 23-27. D. Reidel Publishing Company, 313-326.
- Komhyr, W.D., Barnes, R.A., Brothers, G.B., Lathrop, J.A. and Opperman, D.P. 1995. Electrochemical concentration cell